167

SATELLITE & MESOMETEOROLOGY
RESEARCH PROJECT

Department of the Geophysical Sciences
The University of Chicago

THE CABOT, ARKANSAS TORNADO OF MARCH 29, 1978

by

Gregory S. Forbes
The University of Chicago

SMRP Research Paper 167
August 1978

THE CABOT, ARKANSAS TORNADO OF MARCH 29, 1976

by

Gregory S. Forbes
The University of Chicago

SMRP Research Paper No. 167
August 1978

THE CABOT, ARKANSAS TORNADO OF MARCH 29, 1976

Gregory S. Forbes

ABSTRACT

The Cabot tornado appears to be a classic example of an unsteady tornado. Both the shape of the tornado and the character of the damage path underwent rapid fluctuations. The path of the tornado core exhibited a sinusoidal nature, with at least six "crests". Near the end of the path there appeared to be spectacular weakenings and re-formations of the vortex core, in a pattern resembling a miniature tornado family. The weakenings and reformations appeared to be related to "insurges" from the south side of the tornado, perhaps related to downbursts. In addition, visible suction vortices were present, corresponding to observed swaths of building damage. Classic suction swaths in vegetated fields were not observed, however, because such fields were not present.

A comparison of tornado appearance and damage, windspeed, and underlying surface is made. There appears to be a basic difference in the appearance of the dust and debris cloud related to the nature of the underlying surface: forest, plowed field, grass field, residential area. Other relations are complicated.

Windspeeds were computed photogrammetrically from a tornado movie. The maximum velocity calculated, 63.5 m/s (142 mph) excluding suction vortex rotation, agrees with damage indications that the maximum intensity was no more than F3.

Photogrammetric computation of the vortex tilt at one time indicated that the tornado center at the ground was located 270 m southwest of the center at cloud base.

1. INTRODUCTION

On Monday, March 29, 1976 a tornado ripped through the central business district of Cabot, Arkansas, a small town of about 3500 people. One person was killed in a mobile home park on the southwest edge of town, and four more were killed when a downtown building collapsed. Sixty-four persons were injured. Damages amounted to $8 million, with approximately 250 commercial buildings and residences destroyed or heavily damaged.

The author performed an aerial photographic and mapping survey of the tornado path on Wednesday, March 31, 1976. Professor Ted Fujita also viewed and photographed the path before departing to survey another tornado track. The survey revealed that the tornado touched down about 10.5 miles (17 km) west-south west of Cabot, and about 1.5 miles (2.4 km) north of the western edge of Little Rock Air Force Base. Touchdown time was approximately 1508 CST. The tornado struck Cabot about 1521 CST. After striking Cabot, the tornado made a right turn and moved almost eastward for 6 miles (10 km) before lifting about 1529 CST. The total path length was 16.6 miles (27 km) long. Figure 1 illustrates the tornado path.

There was no evidence that the damage exceeded intensity F3. Much of the strong damage was confined to arc-shaped swaths, and the overall width of the major damage was quite narrow. Minor (F0) damage was occasionally observed to be up to 0.8 mile (1.3 km) wide, however. Because of these sporadic fluctuations in damage width, and because the F-scale was difficult to assess over the open fields and forests, no DAPPLE classification (Abbey and Fujita, 1975) has been attempted. The Fujita-Pearson rating (FPP) was 3, 3, 3.

The tornado appeared to move at approximately 50 mph. Photographs (including two movies) of the tornado were obtained from six persons. These photos covered a substantial portion of the tornado track. One of the movies and three sets of still photos were used extensively in this report.

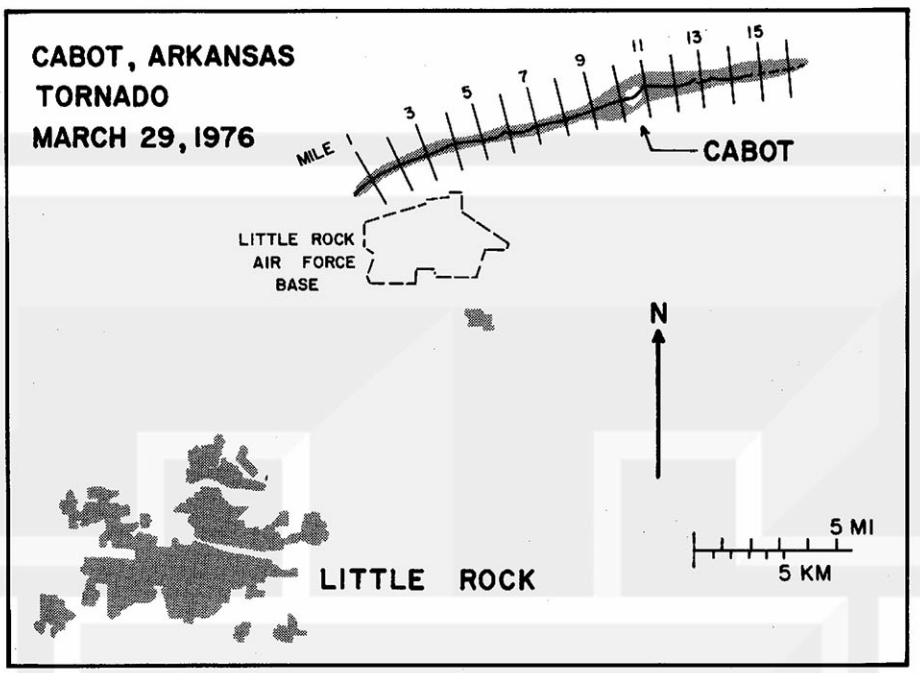

Fig. 1. The Cabot tornado.

The purpose of this report is (1) to compare the rapid changes in tornado appearance with the accompanying damage and windspeeds; and (2) to note the effects of the nature of the underlying surface on the tornado appearance.

2. PHOTOGRAPHIC COVERAGE OF THE CABOT TORNADO

Table 1 lists the sequence of photographic coverage of the Cabot tornado. The photos are listed by the approximate path mile in which they occurred. Additionally, photos by Weaver and a movie by Chapman were not used in this report.

Figures 2 and 3 illustrate the photographers' locations as well as azimuths to the tornado center (at the lowest observable elevation). Also included in these figures are the boundaries of the F0 damage and the swaths of F2 and stronger damage. The F0 boundary is only an approximation, since it is generally difficult to detect damage from 40 mph winds. Therefore, the F0 boundary might really be a better approximation to the average windspeed in the F0 category. The damage path is discussed in detail in Section 3.

TABLE 1

SEQUENCE OF PHOTOGRAPHIC COVERAGE
OF THE CABOT TORNADO

Mile 0 - 1	**Mile 8 - 9**
No Coverage	Cunningham 14
	Beeks Movie 160 - 451
Mile 1 - 2	Gap in Movie
Cunningham A	Cunningham 15
Mile 2 - 3	**Mile 9 - 10**
Cunningham B,C	Beeks Movie 452 - 1093
Ingham 1	Gap in Movie
Mile 3 - 4	**Mile 10 - 11**
Ingham 2,3	Hestir 1 - 5
Miles 4 - 6	**Mile 11 - 12**
No Coverage	Hestir 6 } **
	Beeks Slide 1 }
Mile 6 - 7	
Ingham 4	**Mile 12 - 13**
Cunningham 1,2	Hestir 7 } *
Ingham 5	Beeks Slide 2 }
Cunningham 3-5	Hestir 8 } *
Cunningham 6 } *	Beeks Slide 3 }
Ingham 6 }	
Cunningham 7	**Miles 13 - 17**
	No Coverage
Mile 7 - 8	
Ingham 7-10	
Cunningham 8	* Similar
Cunningham 9 } **	** Identical
Ingham 11 }	
Cunningham 10	
Cunningham 11 } **	
Ingham 12 }	
Cunningham 12,13	
Beeks Movie 1 - 159, Underexposed	

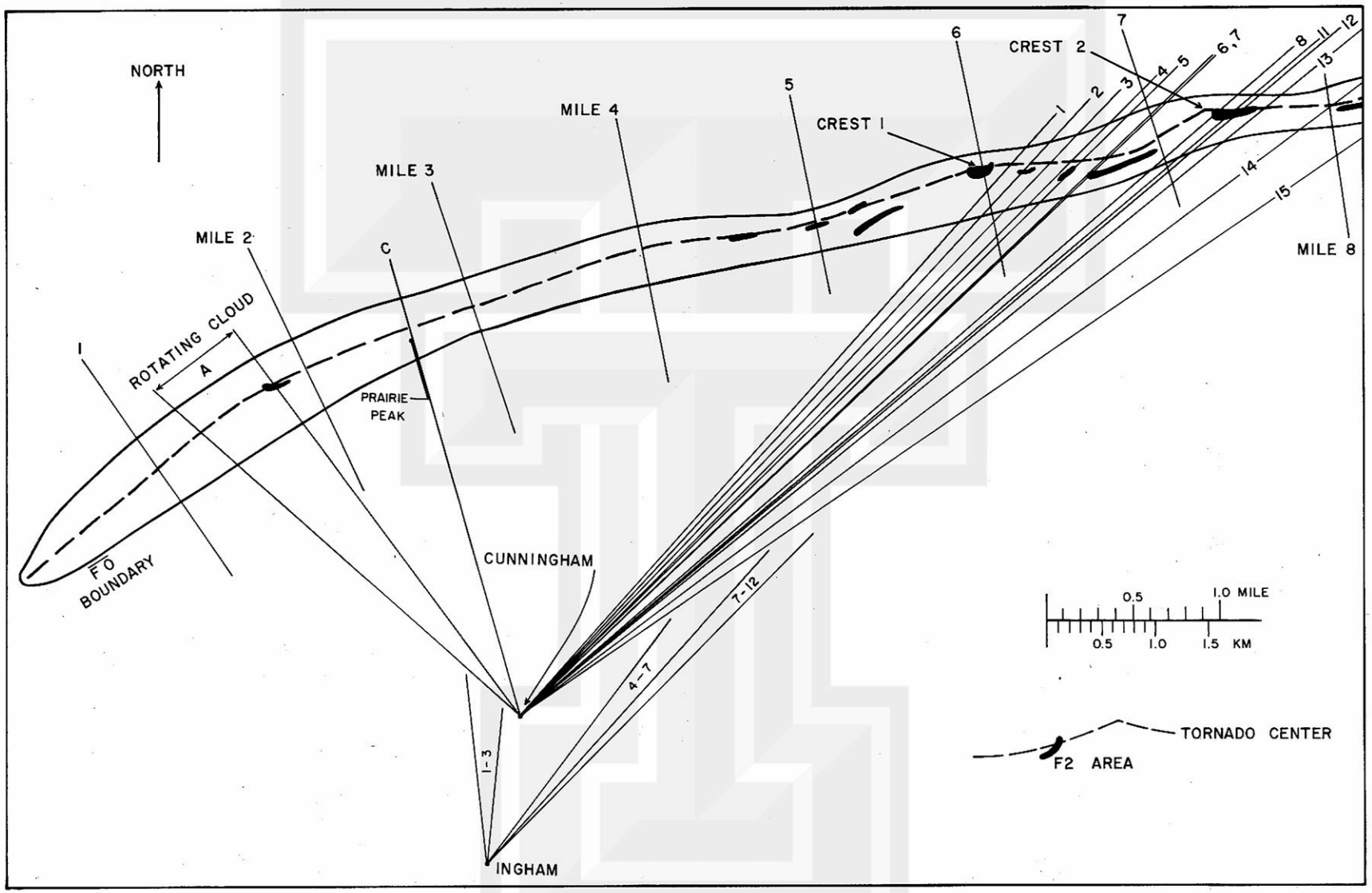

Fig. 2. Cabot tornado track.

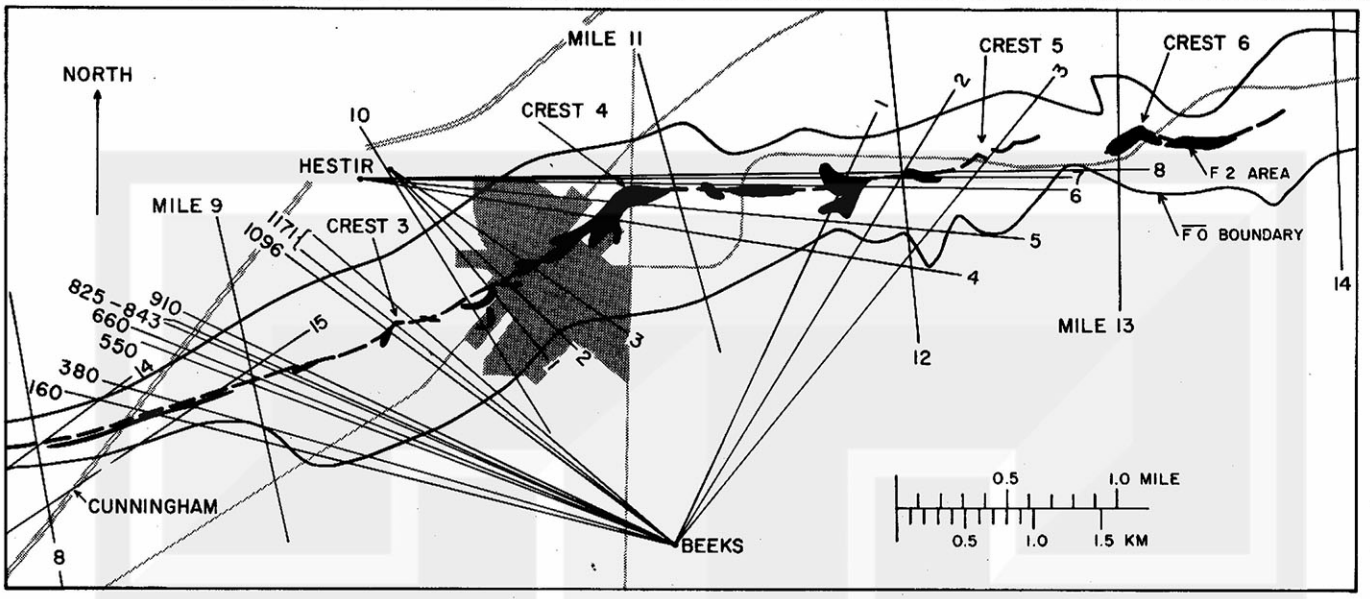

Fig. 3. Cabot tornado track, continued.

James Cunningham took 3 black-and-white (A - C) and 15 color (1 - 15) still photographs of the tornado. Figure 4 is a reproduction of his first photograph. Although the tornado was in progress at this time, no funnel is visible. Only appearing is a spectacular rotating cloud with rainshafts in the background. The width of the rotating cloud (about 0.5 mi or 0.8 km) is shown in Fig. 2.

Figure 5 includes Cunningham's photos C and 1 - 15. Cunningham observed that the tornado was only sporadically visible near the beginning of the track, with changes in appearance even more rapid than sequences A - C and 1 - 5 indicate. After photo 5 the tornado was generally visible, but changed appearance frequently. Robert Ingham's photos showed similar features. Section 5 assesses the possible causes of these changes in appearance.

Donald Beeks took a movie of the tornado as it approached Cabot. Figure 6 reproduces several frames of the movie. Windspeeds computed from the movie are discussed in Section 4.

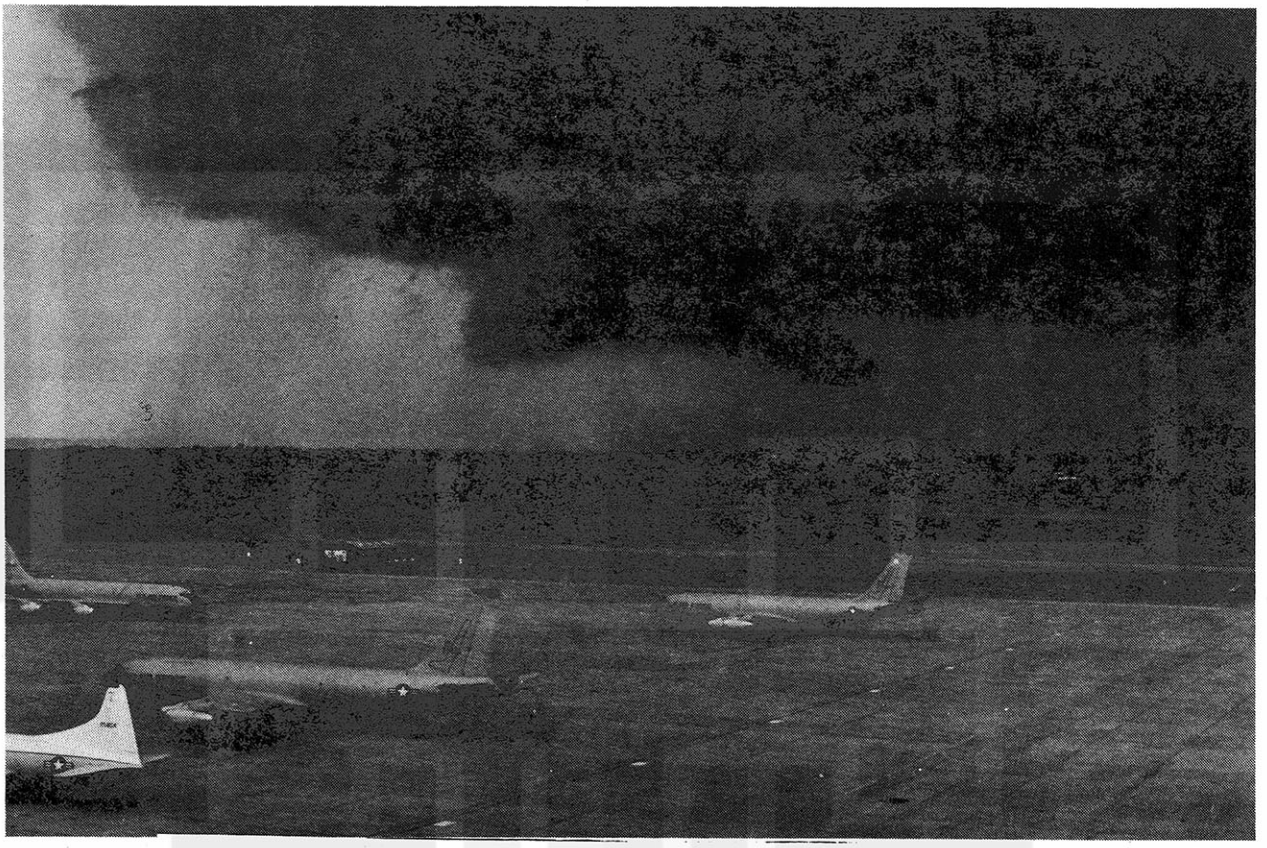

Fig. 4. Cunningham photo (A) of rotating cloud.

The photo sequence in Fig. 6 illustrates the general changes in tornado appearance. Of a spectacular nature are the differences between frames 380 (cylinder) and 550 (dust cloud development) and between 910 and 1096 (disappearance of funnel aloft). There were suggestions of suction vortex presence as early as frame 476, and suction vortices definitely existed after frame 816. Section 5 discusses possible causes of these appearance changes.

Beeks also took three color slides of the tornado after it passed Cabot. The first of these is shown later (Fig. 20) in connection with the photogrammetric calculation of the vortex tilt.

Gary Hestir took seven spectacular color slides of the tornado as it struck Cabot and moved eastward, as reproduced in Fig. 7. Numerous pieces of debris can be seen, along with suction vortices. Photos 1 and 2 suggest the pairing of twin suction vortices, as discussed by Fujita (1975) in the Xenia tornado. These suction vortices correspond to the damage swaths shown in Fig. 14.

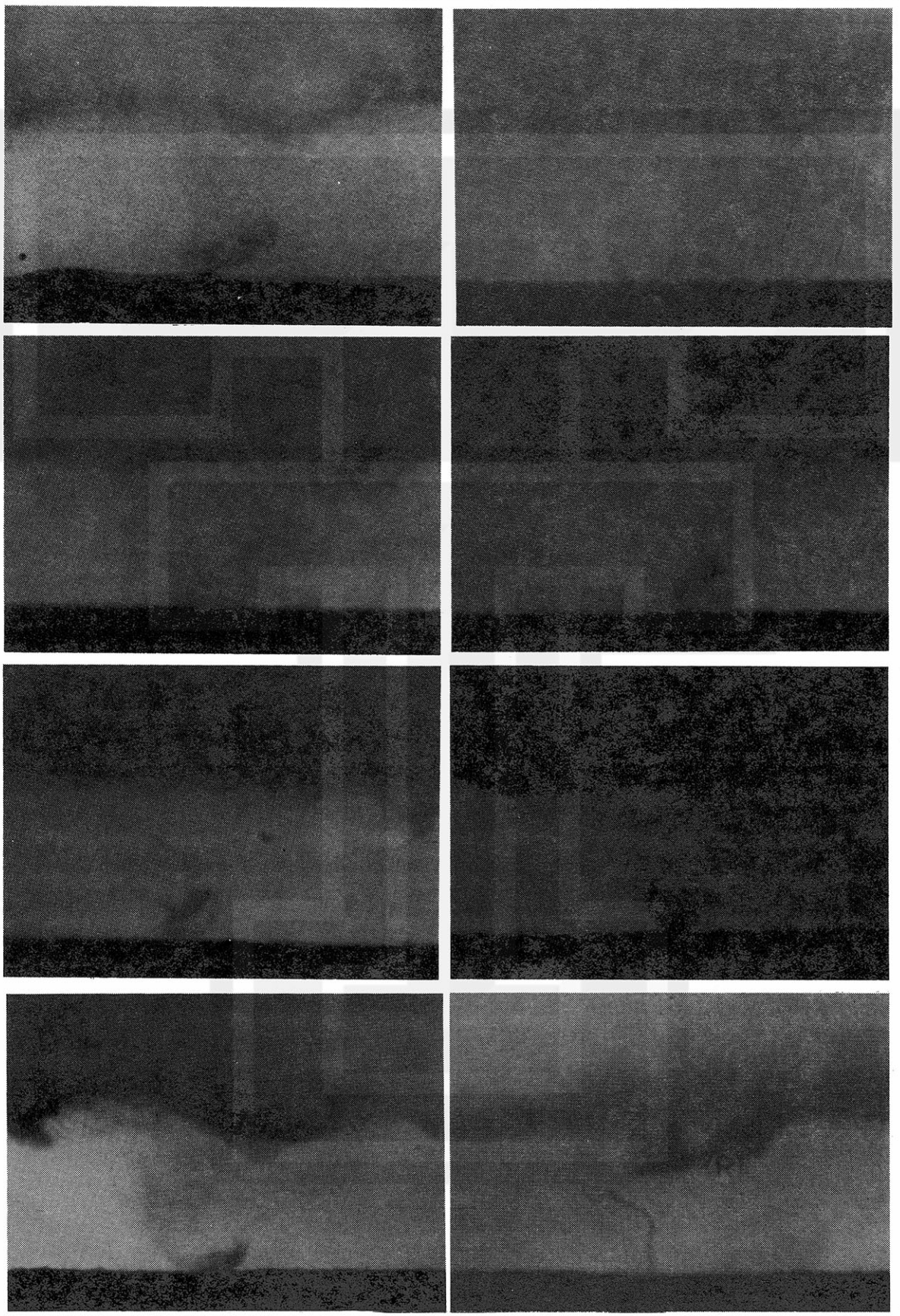

Fig. 5. Cunningham photos.

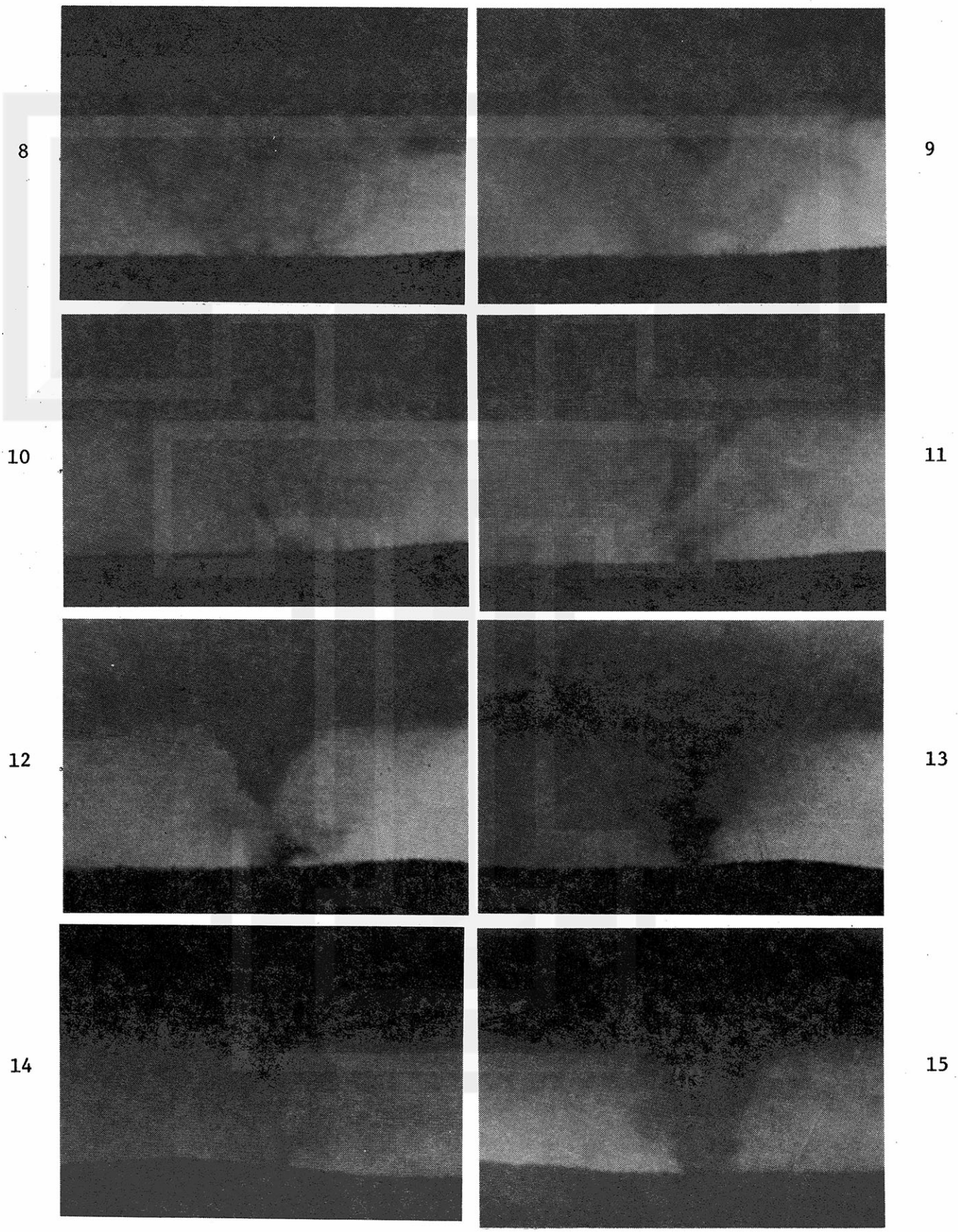

Fig. 5. Cont'd. Cunningham photos.

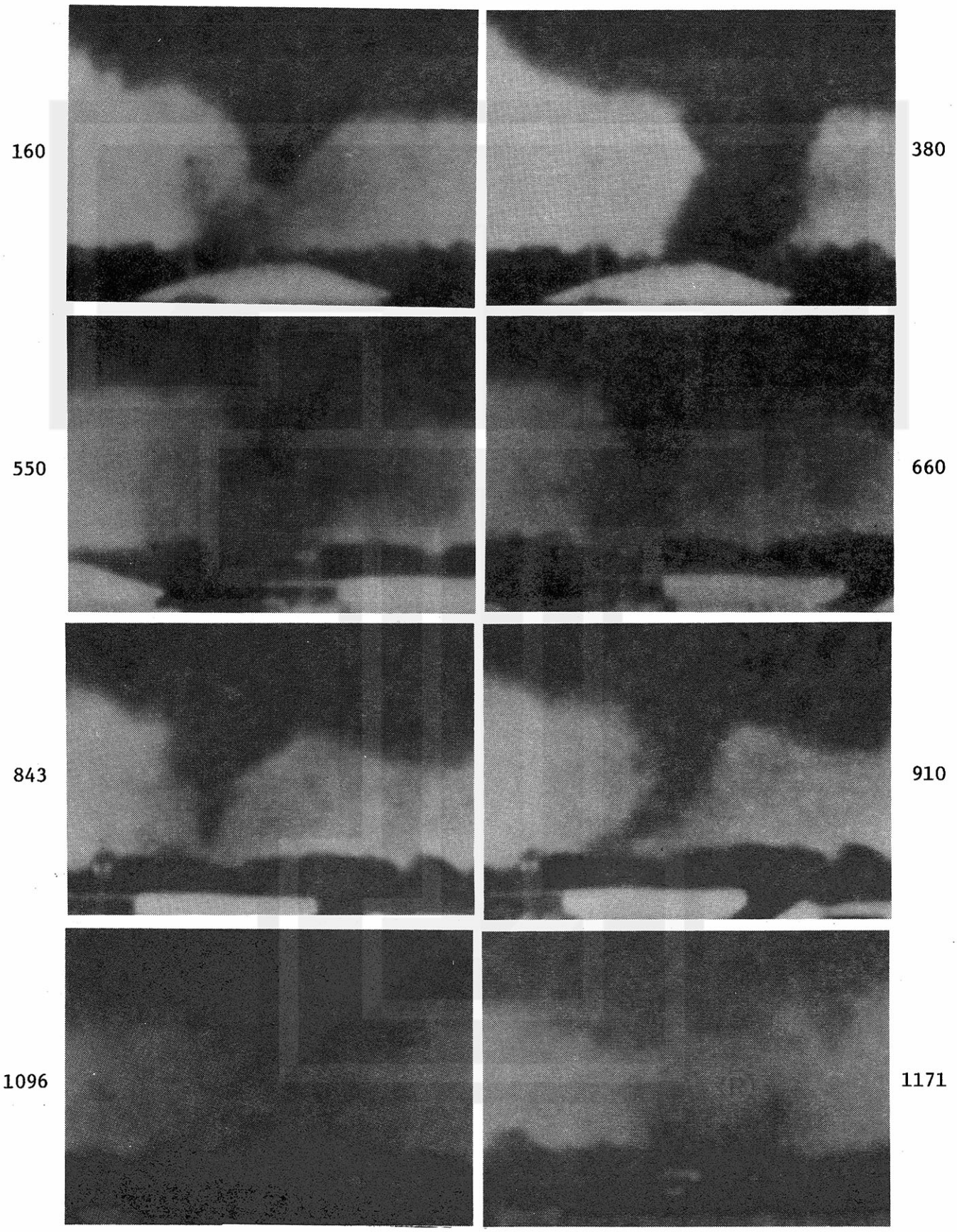

Fig. 6. Beeks photos (from movie).

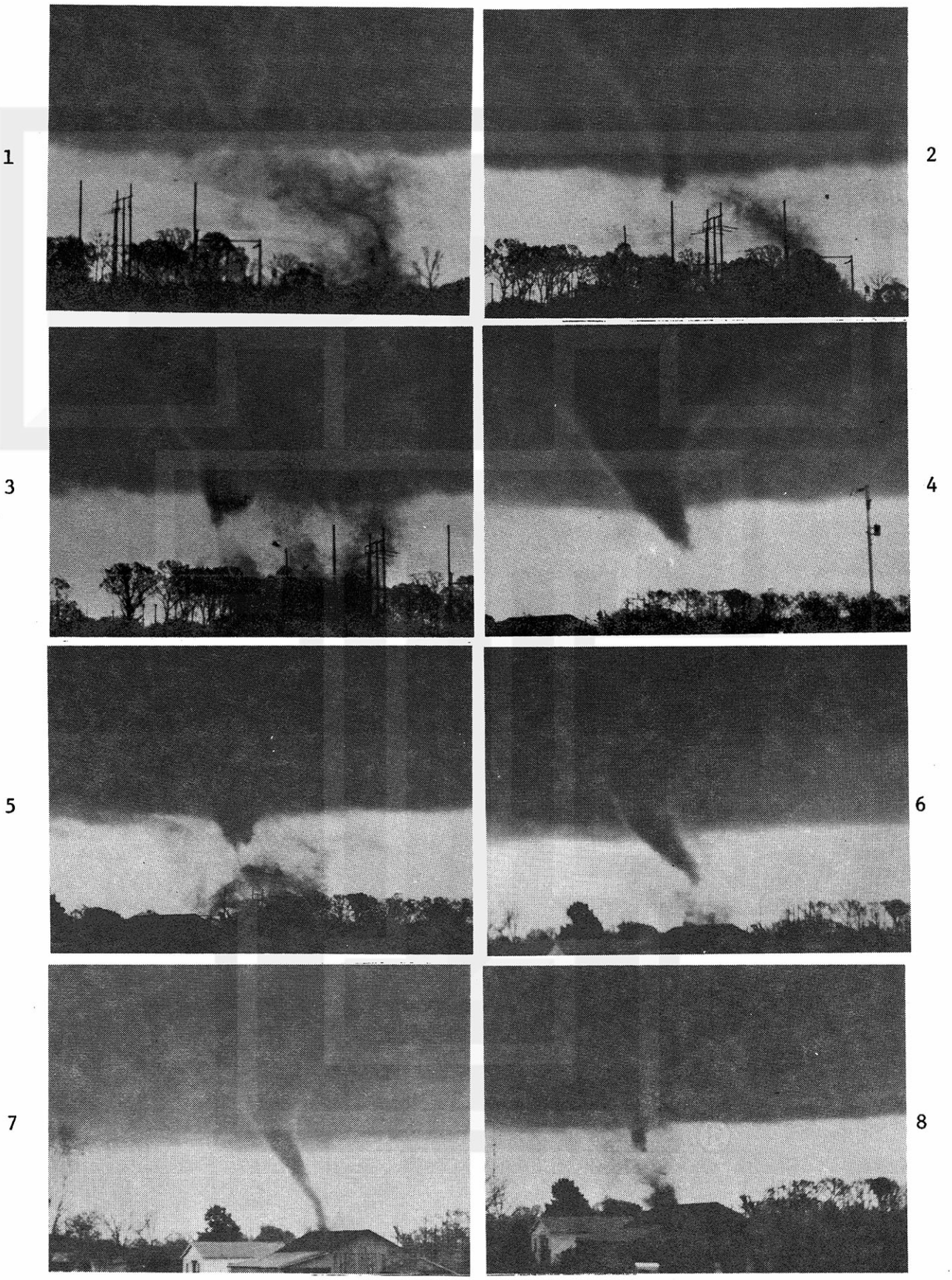

Fig. 7. Hestir photos.

3. DAMAGE PATH OF THE CABOT TORNADO

In addition to aerial photographs taken by the author and by Professor Fujita, the Arkansas Highway Department took 25 vertical, stereographic photos of the path in the vicinity of Cabot (miles 8.8 - 13.8). Thus, an elaborate mapping was available in this region. Locations of tornado photos of Section 2 are shown on the vertical damage photos (Figs. 11, 13, 14, 16, 18, 21, 22).

Damage in miles 0 - 4 was rather weak, perhaps caused primarily by the winds of the rotating cloud (Fig. 4). A concentrated vortex may have been present sporadically, however. Figure 8 suggests that a small vortex passed almost over the two demolished homes.

After mile 5 the tornado generally increased in intensity, frequently causing F2 damage. As was the case later in the tornado, the F2 damage appeared to be confined to occasional swaths rather than a continuous swath. Large open spaces in this region make the conclusion tenuous, however.

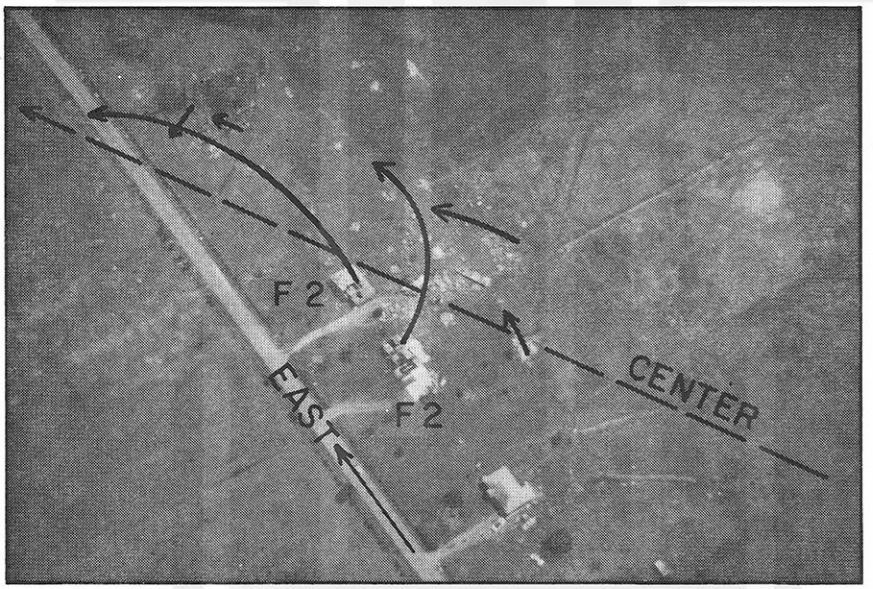

Fig. 8. Tornado damage near mile 1.8.

Figure 2 illustrates that after mile 5 the tornado began to move in a weak sinusoidal pattern. "Crests" occur at approximately miles 6 and 7.3.

Between miles 8.0 and 8.9 the tornado primarily moved through a forested region. The forest was interrupted near mile 8.4 by Interstate 67, and between miles 8.6 and 8.9 the tornado moved along the northern edge of the forest, as shown in Figure 9. A herringbone pattern of tree-fall was observed, particularly after mile 8.3, as illustrated in Figure 10. Refer to photos 14 and 15 of Fig. 5 and frame 160 and 380 of Fig. 6.

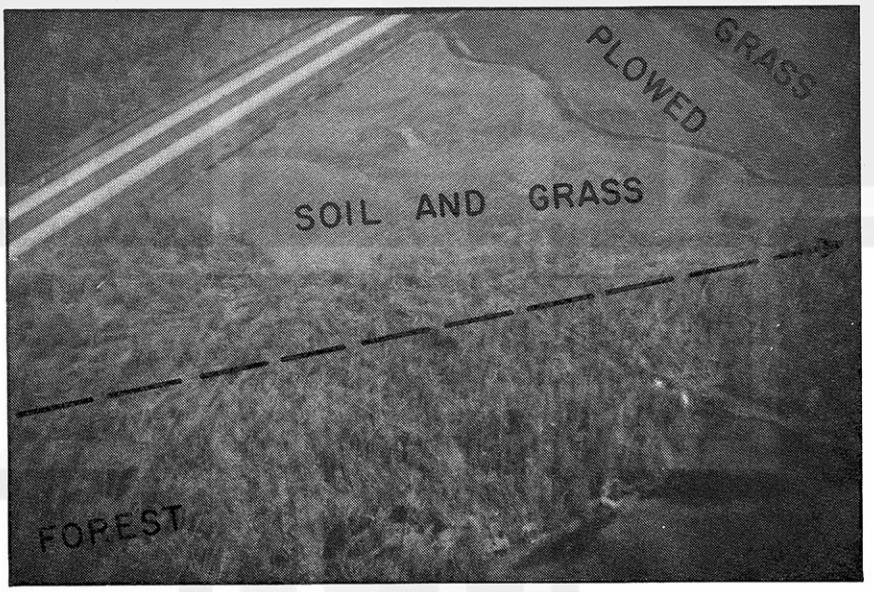

Fig. 9. Movement of the tornado along the northern edge of the forest.

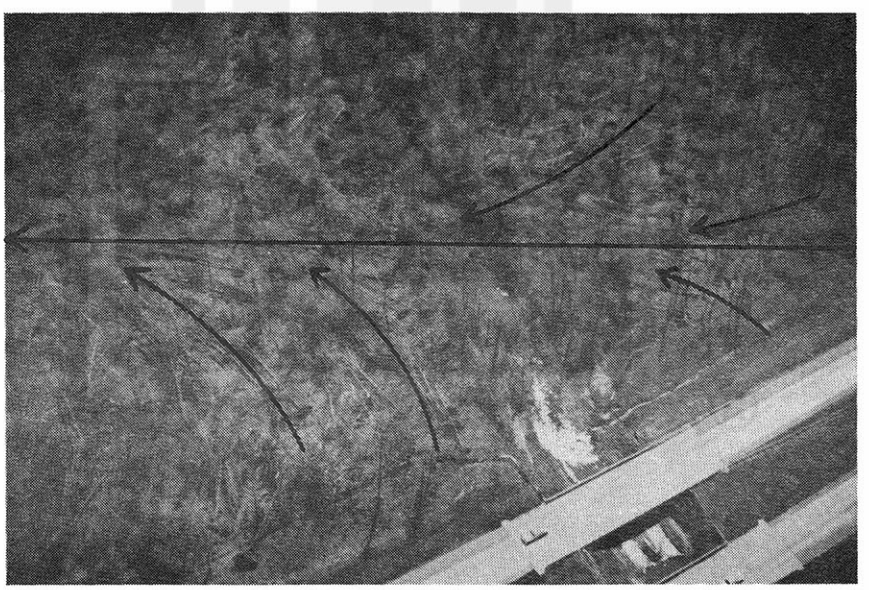

Fig. 10. Herringbone pattern of treefall, as the tornado moved east of Interstate 67. Tornado movement was from right to left, east-northeastward.

Figure 11 illustrates the tornado path after it exited the forest. A house was demolished near mile 9.2, which is shown in a close-up view in Fig. 12. Refer to frame 910 of Fig. 6.

Fig. 11. Tornado path mapped on Arkansas Highway Department photo number 9.

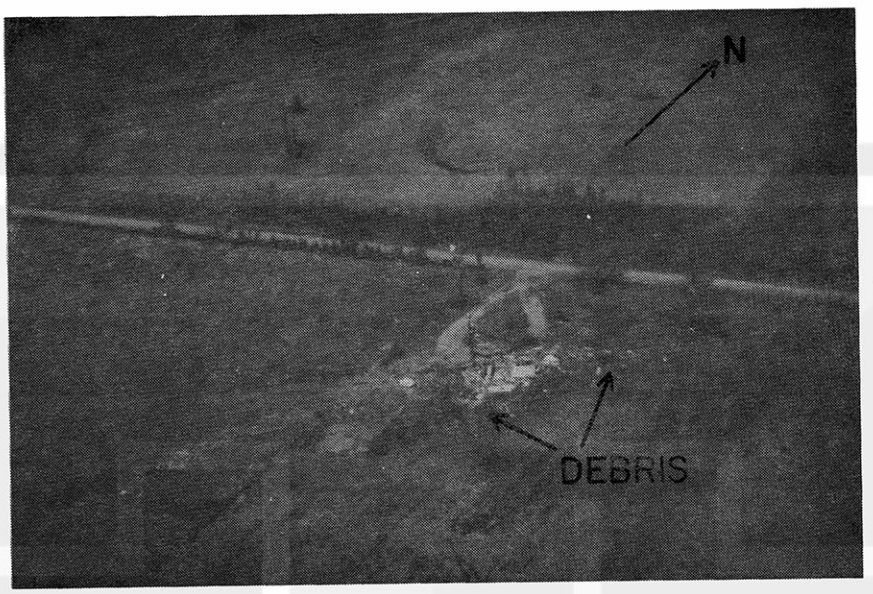

Fig. 12. House demolished near mile 9.2.

The tornado then moved across the grass-field airport, as illustrated in Fig. 13. Loops of debris suggested the presence of suction vortices. Refer to frame 1096 of Fig. 6 which shows a single vortex at 306.3 degrees. Frame 1171 shows suction vortices at 307.6 and 310.0 degrees. The correlation between debris swaths and suction vortices is not obvious, however. Crest 3 in the tornado path occurred here.

Figure 14 illustrates the tornado path through Cabot. One fatality occurred in a mobile home park near mile 10. Figure 15 illustrates the heaviest swaths of damage to the downtown business district where four other persons were killed, near mile 10.25. Two of the apparent suction vortices in photo 3 of Fig. 7 seem to correspond to these swaths.

Figure 16 illustrates the tornado path as the tornado exited Cabot. The tornado made a broad right turn near mile 11 (Crest 4). In recent studies of tornadoes and their environment, the author has observed that such turns are often the result of a strong thunderstorm outflow, referred to as a downburst. (Refer to Fujita, 1978 for illustrations.) For example, one might expect a strong northerly flow on

the north side of the tornado near the right turn. In this case, however, careful analysis of the Arkansas Highway Department photos in that region failed to reveal such a flow. Instead, a broad and diffluent pattern of northerly and northwesterly winds was detected on the south side of the tornado path (mile 10.8 - 11.2).

Fig. 13. Tornado path mapped on Arkansas Highway Department photo number 11.

Between mile 10.8 and 11.2 the tornado left a litter line along the location of confluence of debris trajectories from sources north and south of the litter line. The debris appeared to be primarily lumber from demolished houses, as shown in Fig. 17. The litter line is reminiscent of the line of deposition of corn stubble which marks the right side of the core of a tornado containing suction vortices.

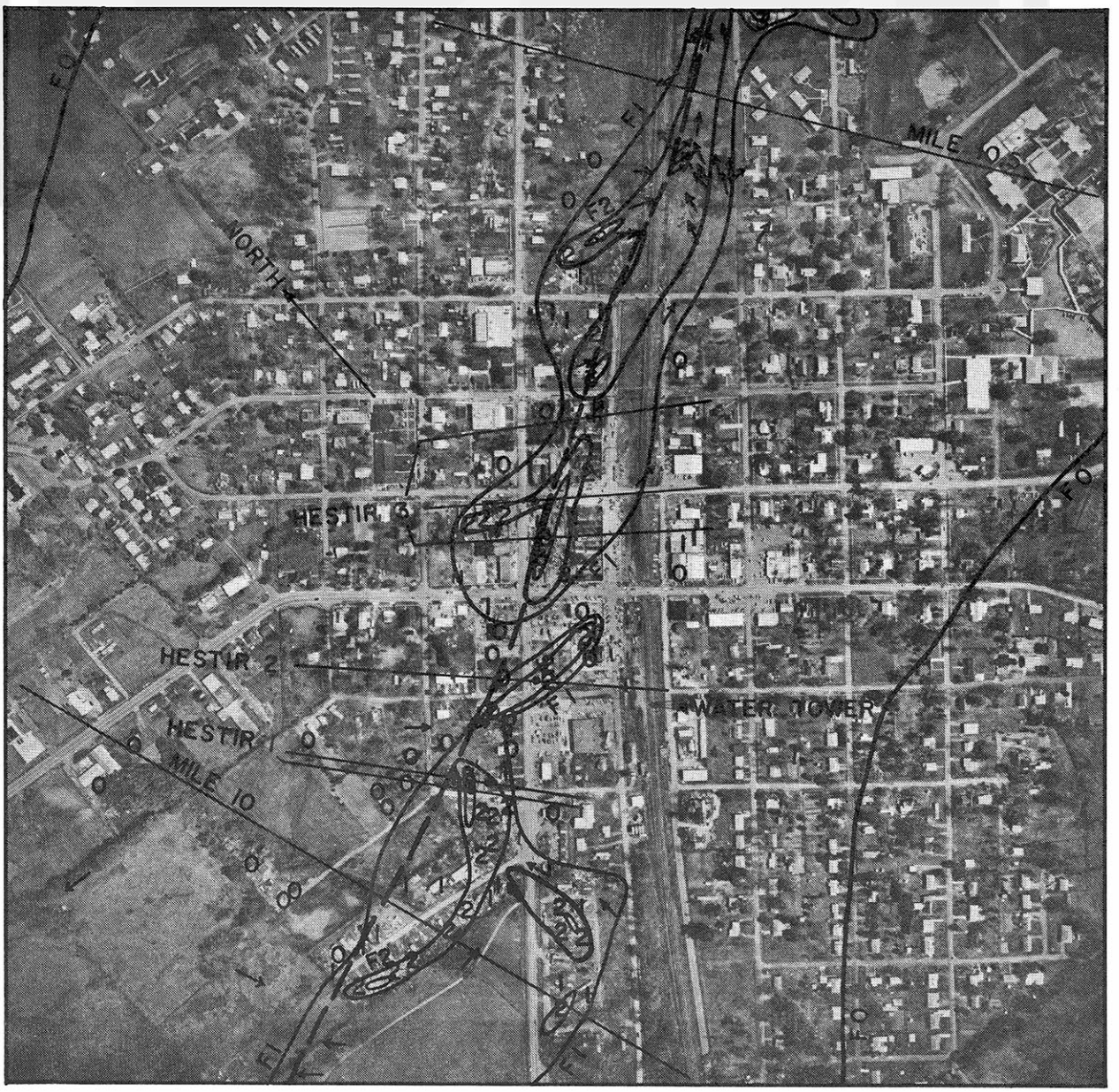

Fig. 14. Tornado path mapped on Arkansas Highway Department photo number 4

Fig. 15. Swaths of F2 and greater damage in downtown Cabot.

Fig. 17. Litter line of deposited lumber near mile 10.9.

Near mile 11.6 there seemed to be an intensification of the tornado. This was revealed in a broad damage pattern involving mobile homes and trees. Two broad swaths of damage are evident in Figure 18: one swirling from the northwest and the other from the west-southwest. Figure 19 is a close-up of some of the damage in the northern swath. There appears to be circulation within the swath, suggesting a suction vortex origin.

Fig. 16. Tornado path mapped on Arkansas Highway Department photo number 15.

Hestir's photo 6 of Fig. 7 and Beeks' slide 1 of Fig. 20 were taken when the tornado struck this location. Hestir's photo suggests the presence of suction vortices, and Beeks' photo suggests overall cloud rotation.

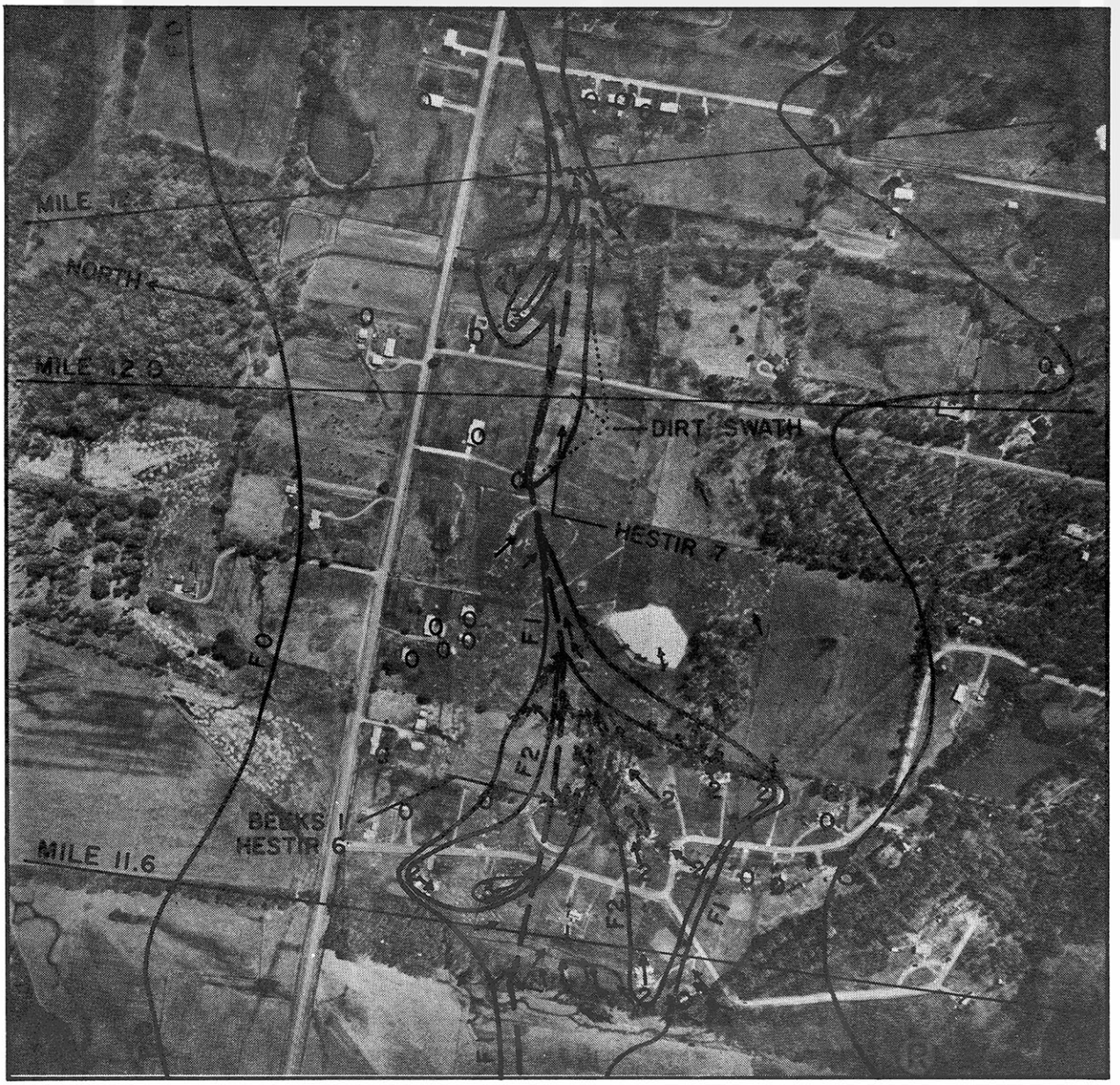

Fig. 18. Tornado path mapped on Arkansas Highway Department photo number 19.

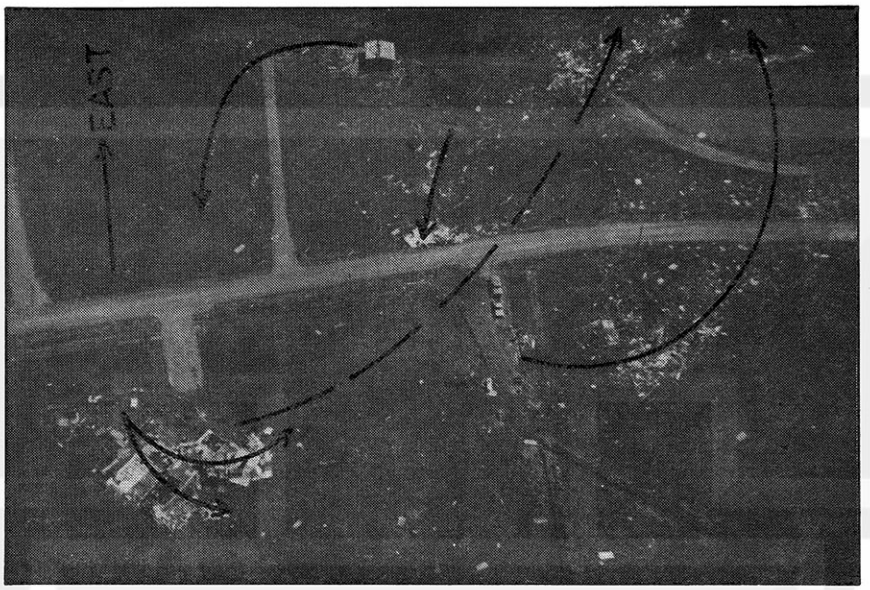

Fig. 19. Mobile homes destroyed in the northern swath near mile 11.7.

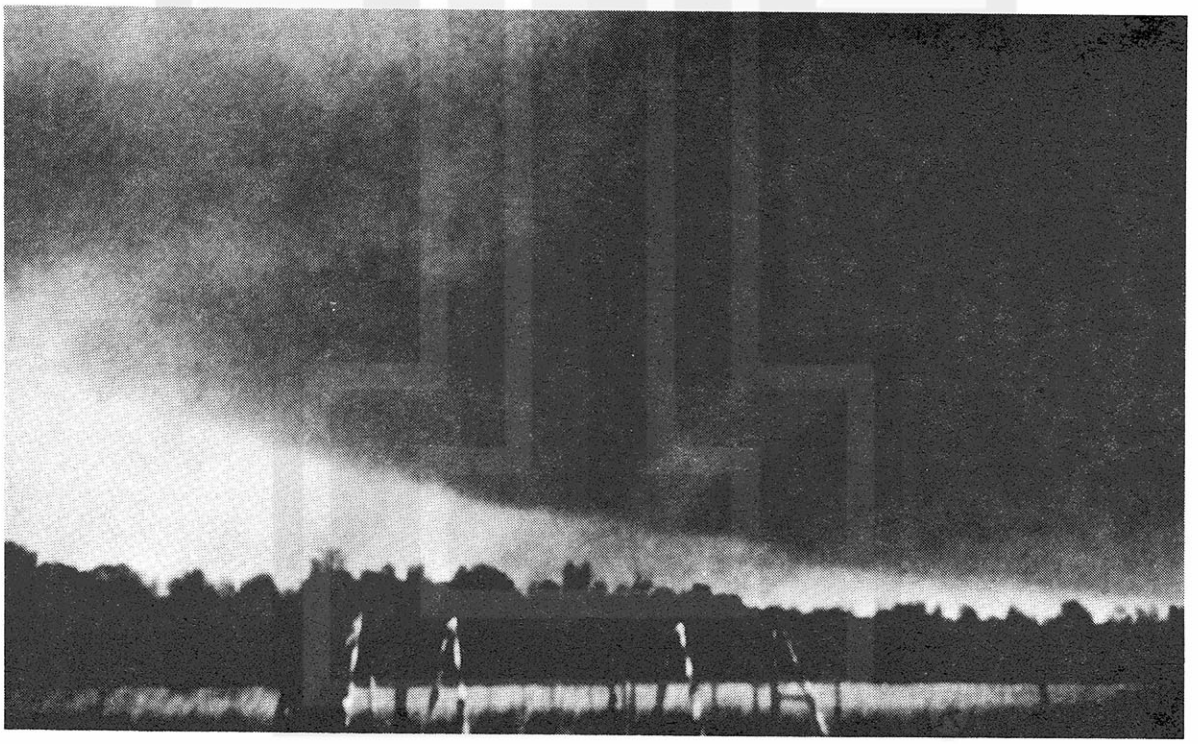

Fig. 20. Beeks' slide 1.

The nature of the tornado appeared to change abruptly near mile 11.8, as the damage path became narrow. A swath of dirt was deposited from near mile 11.9 to mile 12.1. A close-up of the dirt swath is shown in Fig. 21. Refer to number 7 of Fig. 7 for the tornado appearance at this time. Notice that the funnel has become elongated and cylindrical, without indication of suction vortices.

Figure 22 illustrates that the tornado began to become less organized after mile 12.2. The core momentarily disappeared near crest 5, and fully disappeared near mile 12.7. These disruptions may be related to strong southerly flows on the south side of the tornado near miles 12.5 and 12.8, which might be termed downbursts.

The vortex core reappeared near mile 12.9 and formed crest 6 near mile 13.1, as illustrated in Fig. 23. Figure 24 is a close-up of crest 6.

The core was again disrupted, near mile 13.7. Again the disruption was accompanied by a strong southerly flow. After mile 13.7 the tornado remained rather indistinct. The above series of disruptions and reformations of the vortex core resembles a miniature tornado family.

Fig. 21. Dirt swath near mile 12.0.

Fig. 22. Tornado path mapped on Arkansas Highway Department photo number 21.

Fig. 23. Tornado path mapped on Arkansas Highway Department photo number 21.

Fig. 24. Crest 6 near mile 13.1.

4. PHOTOGRAMMETRIC CALCULATIONS OF TORNADO WINDSPEED AND STRUCTURE

Tornado windspeeds were calculated from one-second movie loops prepared from the Beeks movie. Loops were prepared for numerous locations along the tornado path. Figures 25-29 illustrate the windspeeds computed from five of these loops. Indicated velocities are "raw" velocities, computed as if each tracer or "tag" was at the same distance from the photographer as the tornado center. None of the corrections discussed by Fujita (1976) and Forbes (1976, 1978) have been performed, primarily because the tornado appears to defy classification as axisymmetric.

The reader is cautioned that without such corrections the velocities could be in error by as much as 10%. The reader should also keep in mind that the horizontal velocity component is the component of the vector sum of tangential, radial, and translational velocities parallel to the image plane.

Table 2 lists the maximum raw velocity observed in each loop and the average image plane translation velocity. The maximum observed velocity was 63.0 m/s (141.1 mph), and did not include suction vortex rotation. This falls into category F2. Velocities were rarely detectable below 100 m due to obstructions.

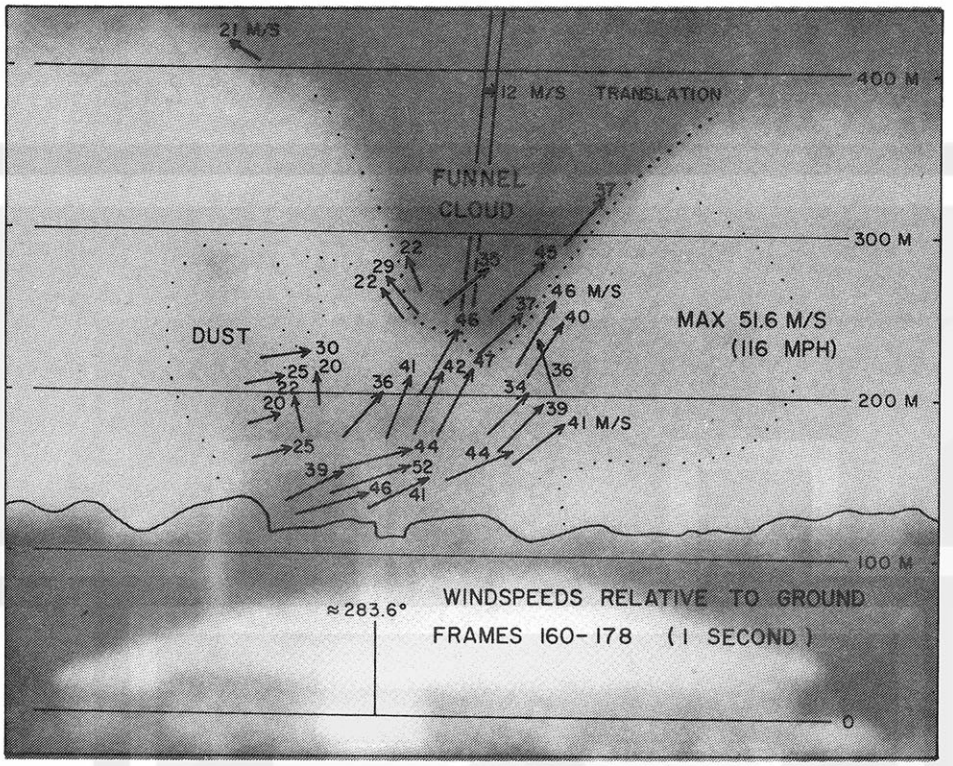

Fig. 25. Windspeeds from frames 160 - 178 of the Beeks movie.

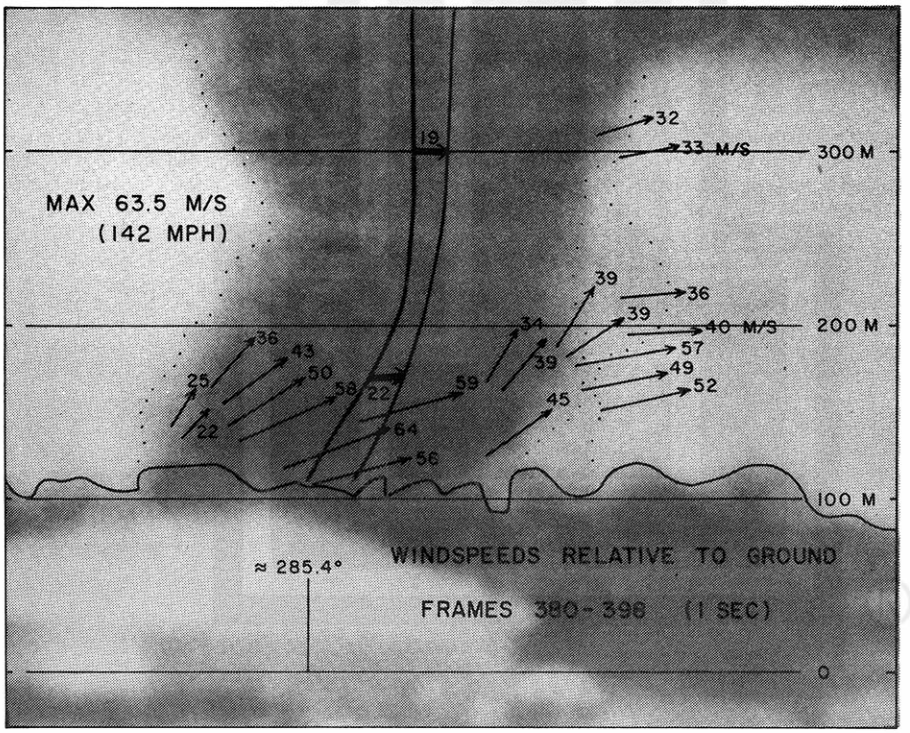

Fig. 26. Windspeeds from frames 380 - 398 of the Beeks movie.

TABLE 2

IMAGE-PLANE VELOCITY COMPONENTS

Frame	Maximum Raw Velocity		Translation
160 - 178	51.6 m/s	(115.6 mph)	12 m/s
178 - 196	50.0	(112.0)	9
380 - 398	63.5	(142.2)	21
388 - 406	59.6	(133.5)	9
550 - 568	56.6	(126.8)	30
558 - 576	53.8	(120.5)	26
660 - 678	61.1	(136.9)	25
664 - 682	63.0	(141.1)	25
825 - 843	54.8	(122.8)	11
835 - 854	56.6	(126.8)	16
825 - 854			13
910 - 928			18
918 - 936			20
990 - 1008	53.4*	(119.6)*	31
998 - 1016	61.2*	(137.1)*	21
OVERALL	63.5**	(142.2)**	19 m/s***

* Few vectors.

** Does not include suction vortex rotation.

*** Implies actual translation of 30 m/s (67 mph).

The average translation was 19 m/s (43 mph). The translation and image plane were typically at a 50 degree angle, implying actual translation of roughly 30 m/s (67 mph). This exceeds the estimate (50 mph) based upon the touchdown time and the time the tornado struck Cabot.

The possible relation between tornado appearance and windspeed is discussed in Section 5.

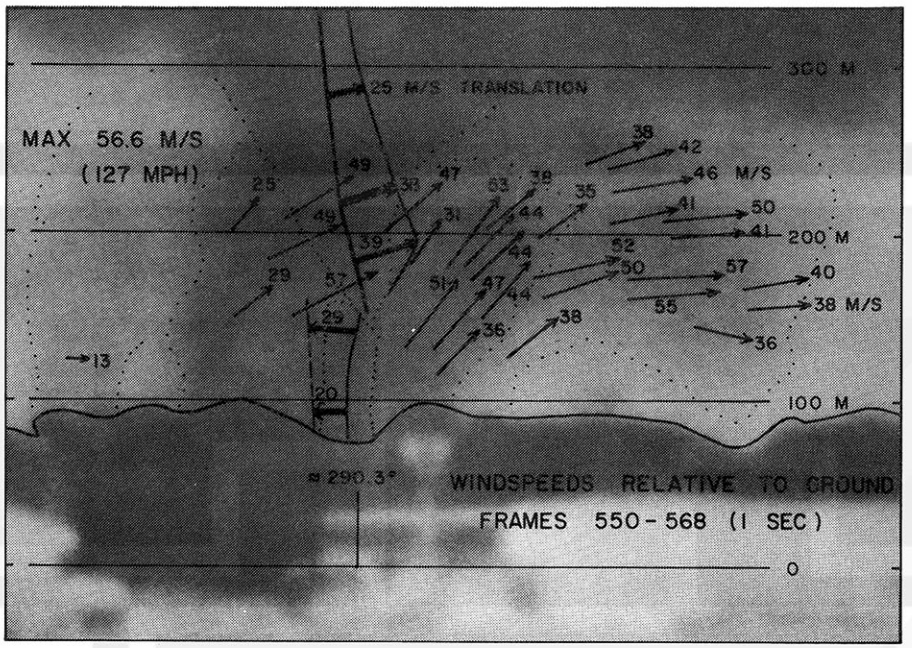

Fig. 27. Windspeeds from frames 550 - 568 of the Beeks movie.

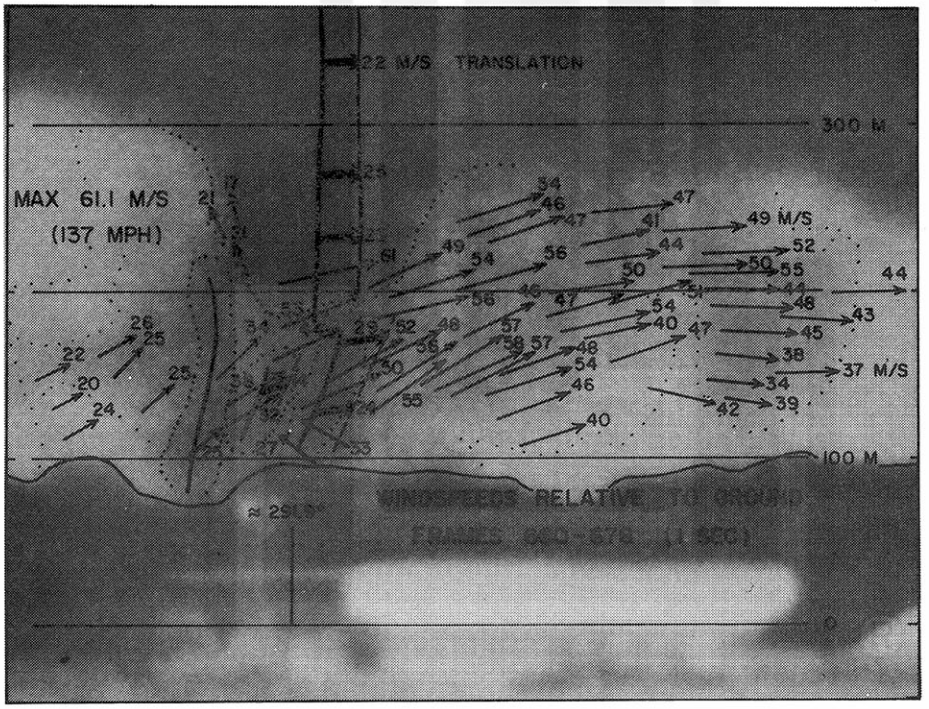

Fig. 28. Windspeeds from frames 660 - 678 of the Beeks movie.

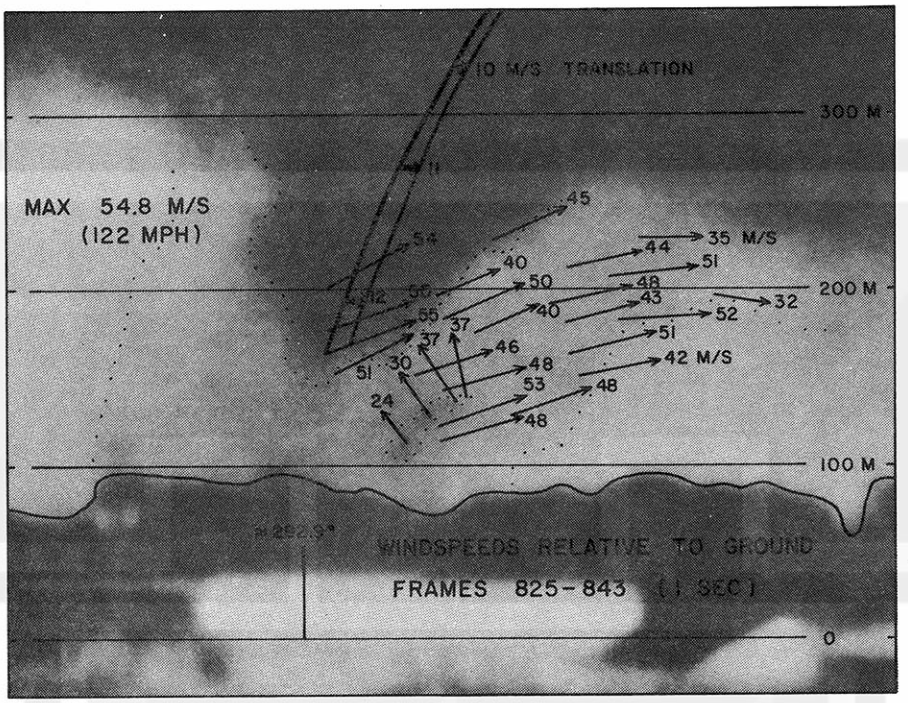

Fig. 29. Windspeeds from frames 825 - 843 of the Beeks movie.

Figures 27 and 28 reveal that a spectacular dust cloud has formed since Fig. 26. The dust cloud formed as dust was picked up over a plowed field. Just prior to Fig. 28 the tornado left the plowed field and lost its dust source. This may explain the decrease in apparent vertical velocity between Fig. 27 and 28 in the region below the funnel cloud: there were now no tracers in the region of strongest vertical velocity where the dust is normally picked up. Instead, we are now viewing leftover dust, perhaps at a different radius. Thus, a temporary source of tracers can lead to rapid changes in the tornado appearance.

Also note in Figs. 27 and 28 that there appears to be a significant contribution to the apparent horizontal velocity from radial (outward) motion in the dust cloud.

Figure 30 illustrates the tilt of the tornado near mile 11.7, by projecting the funnel axis onto the earth's surface. The axis of the tornado at the ground was located about 270 m southwest of the axis at cloud base. The tilt was determined photogrammetrically from photo 6 of Fig. 7 and Fig. 19.

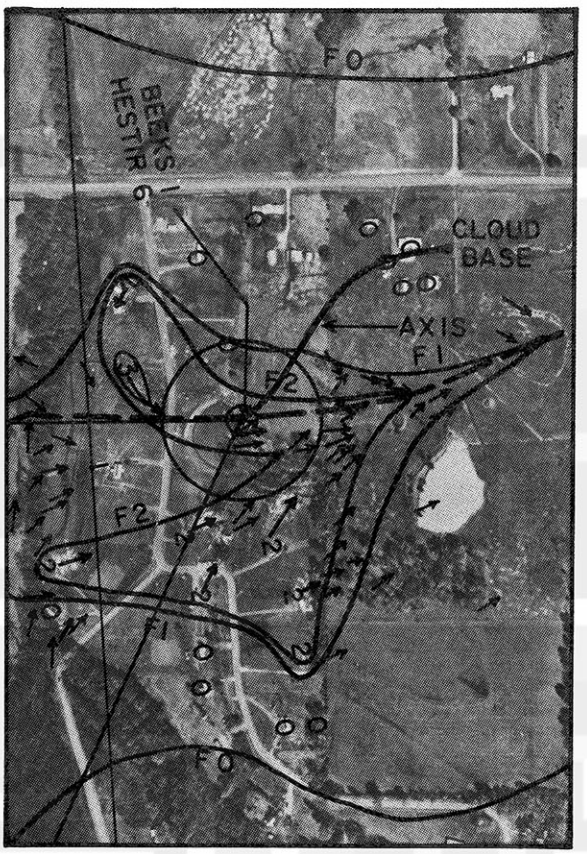

Fig. 30. Photogrammetry of the tornado tilt.

5. POSSIBLE CAUSES AND EFFECTS OF CHANGES IN TORNADO APPEARANCE

This section discusses the possible relations between tornado appearance, damage patterns, windspeed, and nature of the underlying surface.

5.1 Appearance and Damage

There was at least one instance when a dramatic change in tornado appearance was marked by a dramatic change in the damage pattern. This difference is revealed between photos number 6 and 7 of Fig. 7 where the cylindrical funnel elongates and the dust cloud and the suggested suction vortices weaken. This change was accompanied by a transition from a broad core with swaths to a narrow core with a narrow dirt swath (Fig. 18).

Suction vortices corresponded well to swaths of building damage. Refer to photos 1 - 3 of Fig. 7 and Fig. 14. Suction vortices did not correspond well to loops of debris detected on the airport property (frames 1096 and 1171 of Fig. 6 and Fig. 13).

5.2 Appearance and Windspeed

There was no indication that windspeeds above 100 m changed as dramatically as the tornado appearance. Table 2 indicates that the maximum windspeed did not fluctuate by more than about 24%. Nevertheless, there were a few possible relations between windspeed and appearance.

The strongest velocities were observed in frames 380 - 398, when the tornado approached a cylindrical appearance. Vertical velocities appeared to be strongest near the bottom tip of the funnel cloud when it was visible. However, these changes may indicate a different radius of tags being viewed rather than a temporal change in tornado structure.

The disappearance of the funnel cloud aloft between frames 910 and 1096 of Fig. 6 may indicate a change in tornado structure corresponding to the permanent development of suction vortices. Compare this with photos 1 - 7 of Fig. 5, which also show no funnel aloft when suction vortices were generally present.

5.3 Appearance and Underlying Surface

The strongest relation appeared to be between the tornado appearance and the nature of the underlying surface. Photo 15 of Fig. 5 and frame 380 of Fig. 6 illustrate the tornado as it crossed the forest of Fig. 9. After exiting the forest and entering a plowed field (Fig. 11), a dust cloud developed rapidly. Refer to frame 550 of Fig. 6. By frame 660 the tornado has just entered a grass pasture and the dust cloud already has begun to disappear near the tornado axis. By frame 825 the dust cloud has largely disappeared.

Over residential areas, explosions of buildings can contribute debris to a dust/debris cloud. As the debris rises, the tornado may appear to have layers, as in photo 5 of Fig. 7.

As was discussed in Section 4, the nature of the underlying surface appears to exert some control over the apparent windspeed. This does not necessarily mean that it alters the actual windspeed distribution, but it can change what we are able to observe. For example, a dust cloud can mask the radius of maximum winds and the existence of suction vortices. In the example presented in Section 4, the apparent vertical velocity decreased rapidly. But it was probably an apparent rather than a real effect, because the dust source had vanished. As a result, there was no new dust to rise and only leftover dust was viewed within the tornado circulation. The region of strongest vertical velocity now apparently had no tracers in it.

In summary, there are indications that tornado structure (as revealed by the damage pattern), windspeed, and the underlying surface each exert an influence upon the tornado appearance. In addition, changes in tornado appearance can result in apparent (but perhaps fictitious) temporal changes in the wind field. Caution must be exercised in directly relating any two of these parameters without considering the others.

Acknowledgements:-

The author wishes to thank Donald Beeks, Allen Chapman, James Cunningham, Gary Hestir, Robert Ingham, and Fred Weaver for use of their photographs and/or movies. The author also wishes to thank the Arkansas Highway Department for use of their aerial damage photos. The assistance of Robert Koch of the Little Rock Air Force Base, and Frank Makosky, MIC, and Charles Coleman of the Little Rock NWSFO is greatly appreciated. The author is grateful for the support of Professor Fujita.

This research was performed under NRC Contract 04-74-239.

REFERENCES

Abbey, R. F., Jr. and T. T. Fujita (1975): Use of tornado path lengths and gradations of damage to assess tornado intensity probabilities. Preprints, Ninth Conf. Severe Local Storms, AMS, 286-293.

Forbes, G. S. (1976): Photogrammetric Characteristics of the Parker Tornado of April 3, 1974. Proc., Symposium on Tornadoes, June 22-24, Lubbock. Texas Tech Univ., 58-77.

Forbes, G. S. (1978): Three Scales of Motions Associated with Tornadoes. Ph.D. Dissertation. The University of Chicago, 359 pp. Also published as NUREG/CR-0363 by the U.S. Nuclear Regulatory Commission.

Fujita, T. T. (1975): New Evidence from April 3-4, 1974 Tornadoes. Preprints, Ninth Conf. Severe Local Storms, AMS, 248-254.

Fujita, T. T. (1976): Photogrammetric Analyses of Tornadoes. Proc., Symposium on Tornadoes. June 22-24, Lubbock. Texas Tech Univ., 43-44.

Fujita, T. T. (1978): Manual of Downburst Identification for Project NIMROD. SMRP Research Paper No. 156, The Univ. of Chicago, 104 pp.